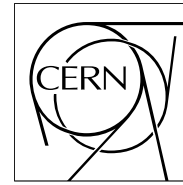


The Compact Muon Solenoid Experiment

# CMS Note

Mailing address: CMS CERN, CH-1211 GENEVA 23, Switzerland



19 October 2003

## Energy Resolution and the Linearity of the CMS Forward Quartz Fiber Calorimeter Pre-Production-Prototype (PPP-I)

A.S. Ayan<sup>1</sup>, N. Akchurin<sup>1,a</sup>, U. Akgun<sup>1</sup>, E.W. Anderson<sup>2</sup>, Z. Bagoly<sup>3</sup>, G.Y. Bencze<sup>3</sup>,  
P. Bruecken<sup>1</sup>, G. Debreczeni<sup>3</sup>, I. Dumanoglu<sup>4</sup>, E. Eskut<sup>4</sup>, A. Fenyvesi<sup>5</sup>, V. Gavrilov<sup>6</sup>,  
A. Gribushin<sup>7</sup>, C. Hajdu<sup>3</sup>, J. Hauptman<sup>2</sup>, A. Kayis<sup>4</sup>, V. Kolosov<sup>6</sup>, S. Kuleshov<sup>6</sup>, J-P. Merlo<sup>1</sup>, M. Miller<sup>1</sup>,  
E. McCliment<sup>1</sup>, J. Molnar<sup>5</sup>, A. Nikitin<sup>6</sup>, Y. Onel<sup>1</sup>, G. Onengut<sup>4</sup>, D. Osborne<sup>8</sup>, N. Ozdes-Koca<sup>4</sup>, V. Pikalov<sup>6</sup>,  
A. Polatoz<sup>4</sup>, I. Schmidt<sup>1</sup>, M. Serin<sup>9</sup>, R. Sever<sup>9</sup>, V. Stolin<sup>6</sup>, A. Ulyanov<sup>6</sup>, A. Umashev<sup>6</sup>, S. Uzunian<sup>6</sup>,  
G. Vesztegombi<sup>3</sup>, D. Winn<sup>10</sup>, A. Yershov<sup>7</sup>, P. Zalan<sup>3</sup>, M. Zeyrek<sup>9</sup>

### Abstract

The first pre-production-prototype (PPP-I) of the quartz fiber calorimeter of the CMS detector has been tested at CERN. The calorimeter consists of quartz fibers embedded in an iron matrix. Results are presented on the energy resolution of the prototype for electrons and pions and the signal uniformity and linearity.

- 
- <sup>1</sup>) University of Iowa, Iowa City, U.S.A.  
<sup>2</sup>) Iowa State University, Ames, U.S.A.  
<sup>3</sup>) KFKI-RMKI, Budapest, Hungary  
<sup>4</sup>) Cukurova University, Adana, Turkey  
<sup>5</sup>) ATOMKI, Debrecen, Hungary  
<sup>6</sup>) ITEP, Moscow, Russian Federation  
<sup>7</sup>) Nuclear Physics Institute of Moscow State University, Moscow, Russia  
<sup>8</sup>) Boston University, Boston, U.S.A.  
<sup>9</sup>) Middle East Technical University, Ankara, Turkey  
<sup>10</sup>) Fairfi eld University, Fairfi eld, U.S.A.  
a) Now at Texas Tech University, Lubbock, U.S.A

# 1 Introduction

Calorimeters are a crucial part of the CMS [1] [2] detector. The hadronic calorimeters will help measure quark, gluon and neutrino directions and energies by determining the energy and direction of particle jets and missing transverse energy. They will also help determine the identification of electrons, photons and muons in conjunction with the electromagnetic calorimeter and the muon detectors. The pseudo-rapidity range of  $\eta < 3.0$  is covered by the HB (Hadron Barrel) and HE (Hadron End-cap) calorimeters. To extend the pseudo-rapidity region to  $3.0 < \eta < 5.0$ , a separate forward calorimeter, HF, is introduced. It is composed of quartz fibers embedded in an iron matrix. It will be located in a region where a very high radiation level will be present.

In 1999, HF collaboration built and tested the first pre-production prototype (PPP-I). The detector was placed on a platform that could move in three dimensions with respect to the H4 beam line of the Super Proton Synchrotron at CERN. The results presented in this paper are on the spatial uniformity, electromagnetic and hadronic energy resolution and the energy response linearity of PPP-I.

## 2 Pre-Production-Prototype I

The PPP-I is an iron absorber matrix with embedded quartz fibers of  $300 \mu\text{m}$  core diameter which serve as the active material. The iron matrix is composed of 2.5 mm thick iron layers with grooves every 2.5 mm. The length of the absorber is 165 cm ( $8.3\lambda_{int}$ ) with a cross sectional area of 18 cm x 18 cm. In each groove, a single quartz fiber is inserted. A total number of 6000 fibers are then grouped into 27 bundles. In PPP-I, there are three different lengths of fibers to achieve a longitudinal segmentation. They are called electromagnetic (EM),  $93.75 X_0$ , hadronic (HAD),  $81.25 X_0$ , and tail catcher (TC),  $17.05 X_0$ . Long fibers sample all shower components while the shorter fibers are biased to the hadron component. The physical spacing between fibers is the 2.5 mm groove spacing. The pattern used for the fiber insertion is shown in Fig. 1. There are two EM fibers for each HAD and TC fiber. PPP-I is divided into nine physical regions called towers, each with a 6 cm by 6 cm cross sectional area (see Fig. 1). At the center of each tower, a radioactive wire source-tube groove exists for calibration. Each fiber bundle (EM, HAD and TC) from a tower is coupled to a separate photomultiplier tube (PMT) via a light-guide and read out as a separate ADC channel.

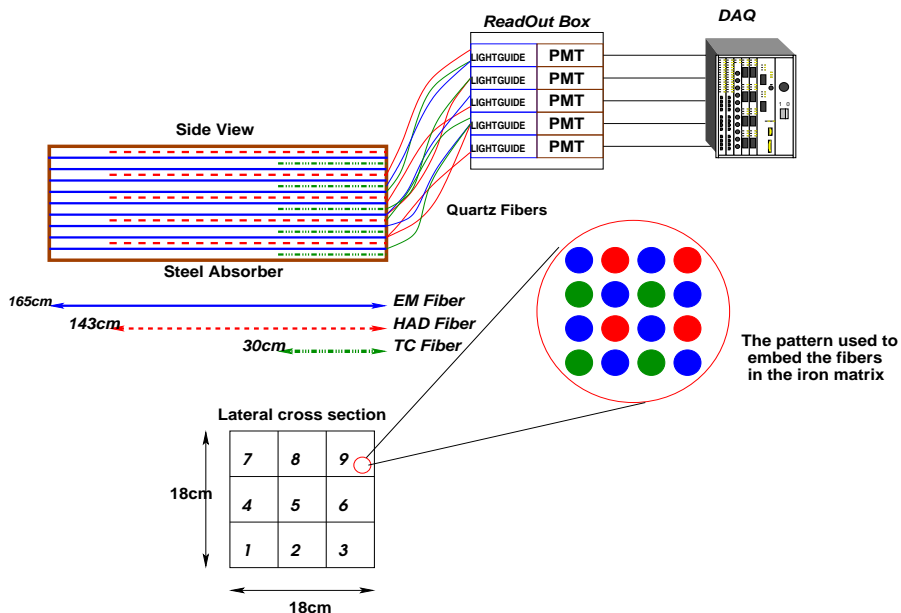


Figure 1: Schematic views of PPP-I.

## 3 Measurements

### 3.1 Spatial Uniformity of PPP-I

One of the factors that effect the calorimeter's response is the non-uniformities in its structure. In PPP-I , this non-uniformity is the granularity of the fibers. When the beam particles enter the detector in an active layer,

i.e. the quartz fiber, the sampling ratio is slightly higher than when they enter in the absorber. Particularly for electromagnetic showers, the shower is concentrated around its axis. So the detector response will have position dependent fluctuations. In PPP-I these fluctuations are in the shape of periodic oscillations which correspond to quartz fiber periodicity as shown below.

In order to study the spatial uniformity of the PPP-I, a 120 GeV electron beam was moved with 1.0 cm steps across the face of the detector and the signals of three adjacent towers (towers 4, 5 and 6. See Fig. 1) were plotted as a function of the beam position. The beam spot size was  $\sim 2$  cm  $\times$   $\sim 2$  cm. With the help of drift chambers located upstream, the impact position of every single particle of the beam on the detector face was known with a precision of  $200 \mu\text{m}$ .

Results of the beam scan are summarized in Fig. 2 and 3. As mentioned earlier, quartz fibers are embedded in the iron matrix as shown in Fig. 1. There are two EM fibers for each HAD and TC fiber giving rise to a 5 mm spacing between two EM fibers. This fiber periodicity can be seen in the beam scan data. The exact EM fiber locations are visible as dark spots in Fig. 2 which plots only the response of the EM fibers with a gray scale as a function of position. In the gray scaled used, the darker color corresponds to higher detector response and vice versa. The white colored area between ( $64 \text{ mm} \leq y \leq 66 \text{ mm}$ ) and ( $54 \text{ mm} \leq x \leq 60 \text{ mm}$ ) in this figure corresponds to a source-tube groove that does not have a quartz fiber so as to allow the insertion of a radioactive wire source for calibration purposes.

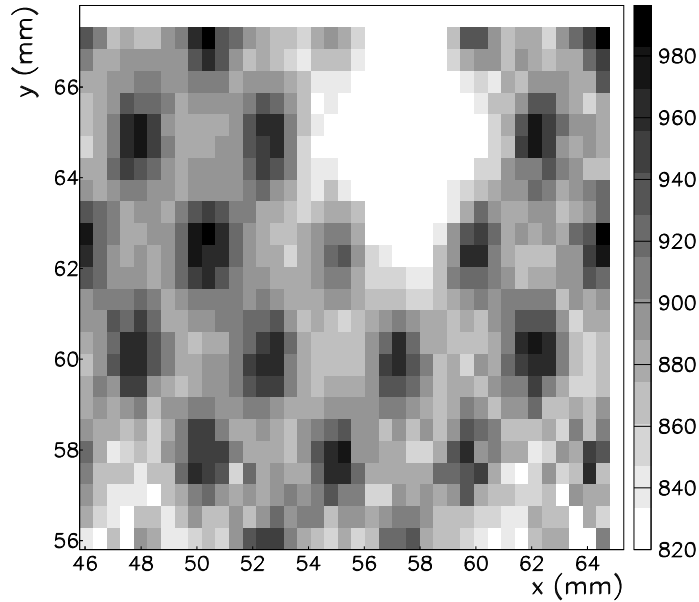


Figure 2: EM fiber locations revealed with 120 GeV electrons. The source tube location is also visible. (See text for details.)

Figure 3 shows the  $x$ -projection of the two dimensional plot shown in Fig. 2 for two consecutive fiber layers. There is a  $\pm 6\%$  fluctuation in the response of the detector due to the fiber periodicity. This is the result of the fact that the response of the calorimeter is slightly higher for particles entering the calorimeter in the fiber plane than for those entering in the absorber plane.

In Fig. 4, the response of the detector is shown for three adjacent towers (4, 5, and 6) as open triangles, squares and circles respectively. As the beam moves from one tower to another, the measured signal amplitudes for adjacent towers change. A sharp tower to tower transition is seen due to the narrow lateral profile of Čerenkov light generating particles. The sum of the signals of three towers is also shown in the same figure as stars with connected line.

A similar beam scan was also carried out with a 120 GeV  $\pi^-$  beam. The  $\pi^-$  beam was moved vertically across the face of the PPP-I. The signal amplitudes are shown in Fig. 5. Since the hadronic showers are not as narrow as electromagnetic ones, tower to tower transition profiles are not as sharp as in the electromagnetic case due to the

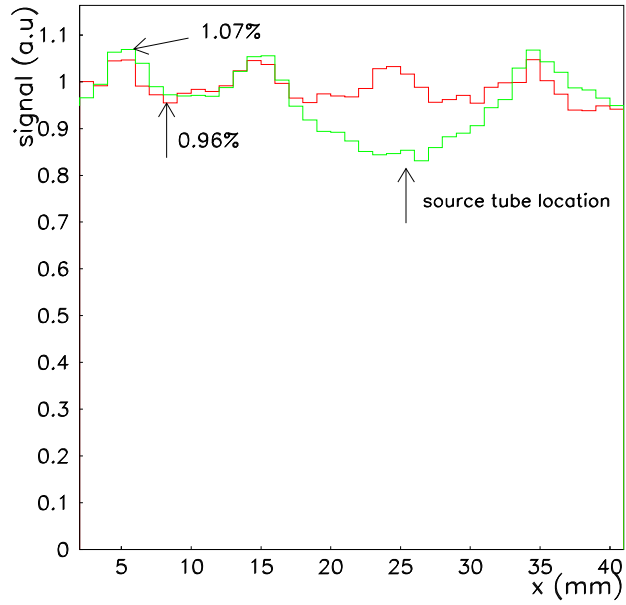


Figure 3: Overlaid  $x$ -projections of Fig. 2 at  $y = 60\text{mm}$  and  $y = 65\text{mm}$

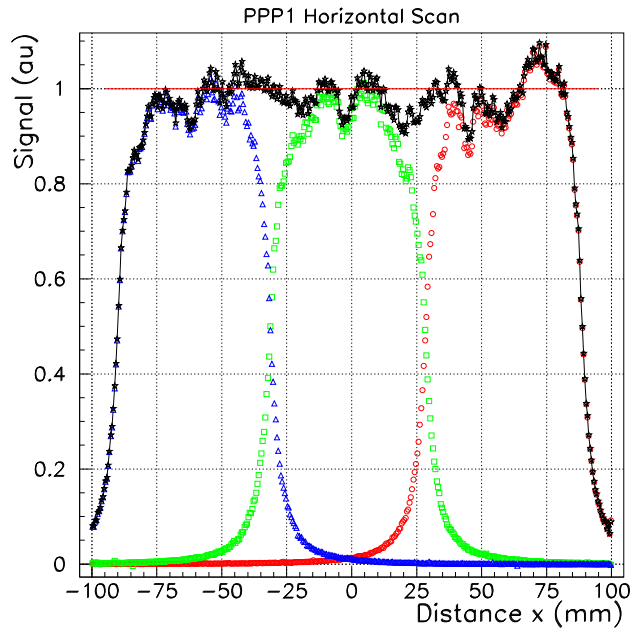


Figure 4: Horizontal scan along towers 4,5,6 (open triangles, squares and circles, respectively) with 120 GeV electrons and the sum of the signals of the three towers (stars connected with line)

larger tails. Therefore the contribution of the adjacent towers to the total signal at a given tower position is higher compared to the electromagnetic case giving rise to a larger total signal.

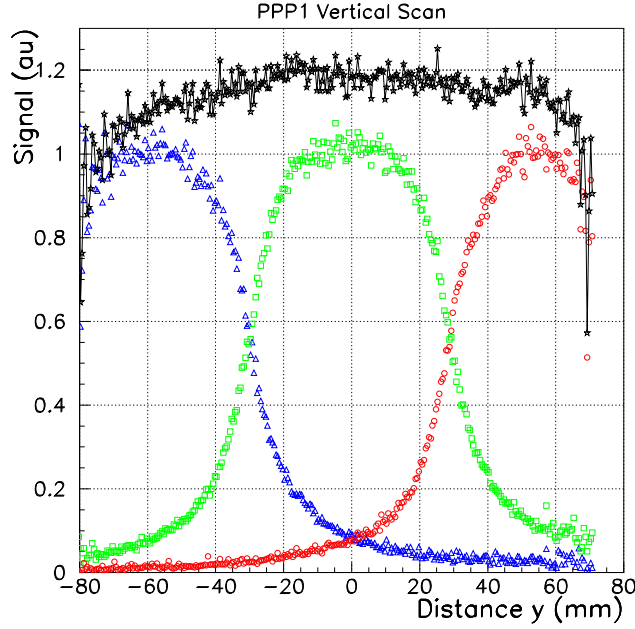


Figure 5: Vertical scan along towers 2,5,8 (open triangles, squares and circles, respectively) with 120 GeV pions and the sum of the signals of the three towers (stars connected with line)

### 3.2 PPP-I Energy Resolution

The energy resolution of a calorimeter, in general, can be parametrized as

$$\left(\frac{\sigma}{E}\right)^2 = \left(\frac{a}{\sqrt{E}}\right)^2 + \left(\frac{b}{E}\right)^2 + c^2 \quad (1)$$

The first term is the sampling term and characterizes the statistical fluctuations in the signal generating processes. The second term corresponds to noise and includes the energy equivalent of electronic noise as well as pileup. The third term is the constant term and is related to the imperfections of the calorimetry, signal generation and collection non-uniformity, calibration errors, and fluctuations in the energy leakage from the calorimeter.

The energy resolution of PPP-I was studied in response to both electron and pion beams at different energies. The beam energies and the particle type used are summarized in Table 1.

Table 1: Beam type and energies used for energy resolution study

Beam	Energy ( $GeV/c^2$ )
$e^-$	6, 8, 15, 20, 35, 50, 80, 100, 120, 150, 200
$\pi^-$	12, 15, 20, 35, 50, 80, 100, 120, 150, 175, 200, 225, 250, 275, 300, 350, 375

It had been shown in one of our earlier prototype tests [6] that in a quartz fiber calorimeter the electromagnetic energy resolution was completely dominated by photoelectron fluctuations. Therefore when we characterize our electromagnetic energy resolution we can drop the noise term to give:

$$\left(\frac{\sigma}{E}\right)^2 = \left(\frac{a}{\sqrt{E}}\right)^2 + c^2 \quad (2)$$

. The response of the PPP-I has been recorded as a function of beam energy. As an example of the typical response of the detector to electron and pion beams, the signals recorded for a 100 GeV electron beam and a 225 GeV  $\pi^-$

beam are shown in Figs. 6 and 7. The response of the calorimeter to electrons is seen to be Gaussian. However a deviation from Gaussian behavior is seen in the response to the  $\pi^-$  beam. This is a result of the different natures of electromagnetic and hadronic showers [3].

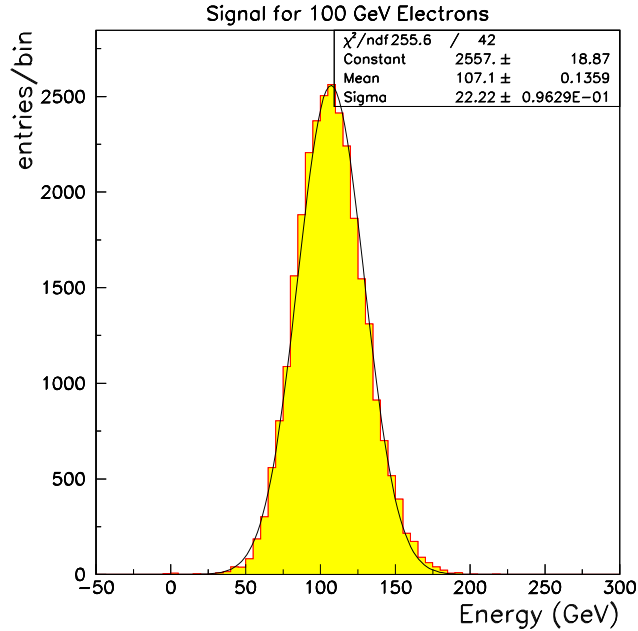


Figure 6: PPP-I response to 100 GeV  $e^-$ s

Of the secondary hadronic particles, mostly  $\pi^0$ s contribute to the Čerenkov signal since they decay into two photons which in turn contribute to the electromagnetic core and register in the detector as Čerenkov light. Other non-electromagnetic secondaries are mostly not relativistic and therefore do not give rise to Čerenkov light and hence do not register in the detector. At low energies, the number of  $\pi^0$ s in the shower is characterized by a Poisson distribution which becomes more and more Gaussian at high energies.

Fig. 8 shows the energy resolution for electrons as a function of energy. The resolution ( $\sigma/E$ ) is plotted against  $1/\sqrt{E}$  and fitted to equation 1. The fit yields

$$\left(\frac{\sigma}{E}\right)^2 = \left(\frac{197\%}{\sqrt{E}}\right)^2 + (8\%)^2.$$

Hadronic energy resolution of PPP-I as a function of energy is shown in Fig. 9. At 1 TeV, the energy resolution is 20%.

### 3.3 Energy Response Linearity

PPP-I exhibits a different response to electromagnetic and hadronic showers. The data sample shown in Table 1 used in this study. The response of the PPP-I was recorded as a function of beam energy. The measured response, then, was normalized by dividing by the beam energy and plotted against the beam energy (Fig. 10 and Fig. 11).

The response as a function of electron beam energy is linear to within 1%. However, as seen in Fig. 11, the response is very non-linear for different energies of hadronic beams. This is due to the electromagnetic portion of the hadronic shower, that is, the  $\pi^0$  content. As the beam energy increases, the  $\pi^0$  fraction increases giving rise to a larger Čerenkov signal in the detector.

## 4 Summary and Conclusions

A Pre-Production-Prototype for the forward calorimeter of the CMS detector has been tested at the H4 beam line at CERN. The electromagnetic energy resolution was measured to be  $\left(\frac{\sigma}{E}\right)^2 = \left(\frac{197\%}{\sqrt{E}}\right)^2 + (8\%)^2$ . The hadronic

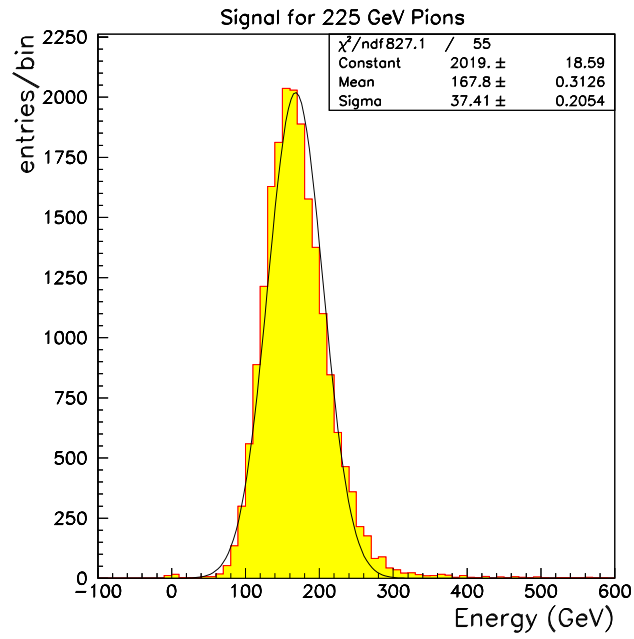


Figure 7: PPP-I response to 225 GeV  $\pi^-$ s

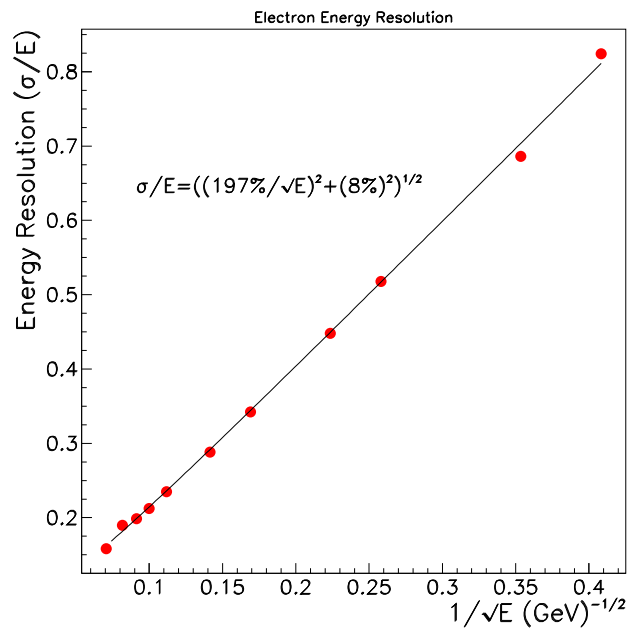


Figure 8: Electromagnetic energy resolution as a function of  $1/\sqrt{E}$

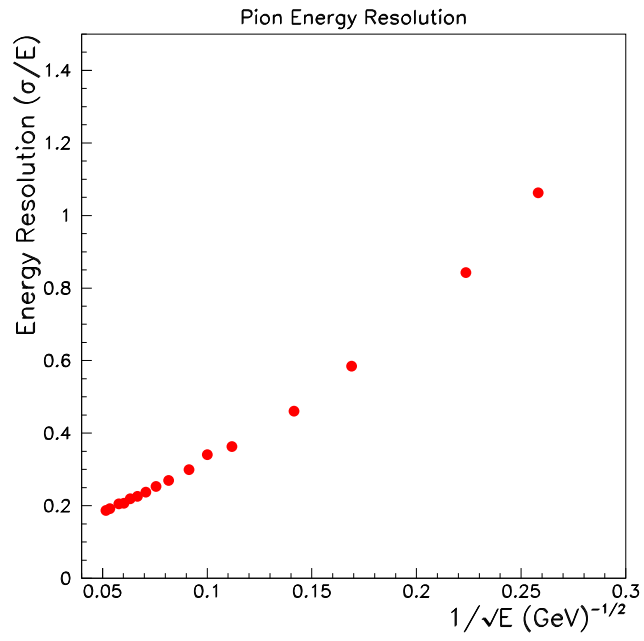


Figure 9: Hadronic energy resolution as a function of  $1/\sqrt{E}$

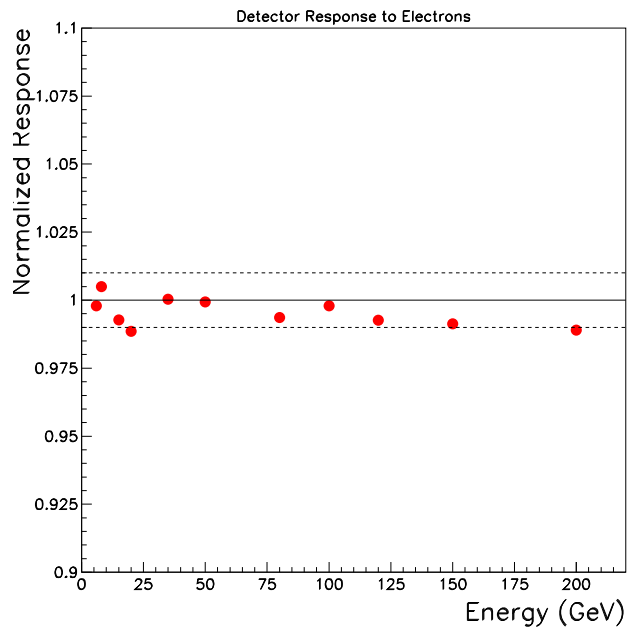


Figure 10: Normalized response to  $e^-$ s as a function of beam energy

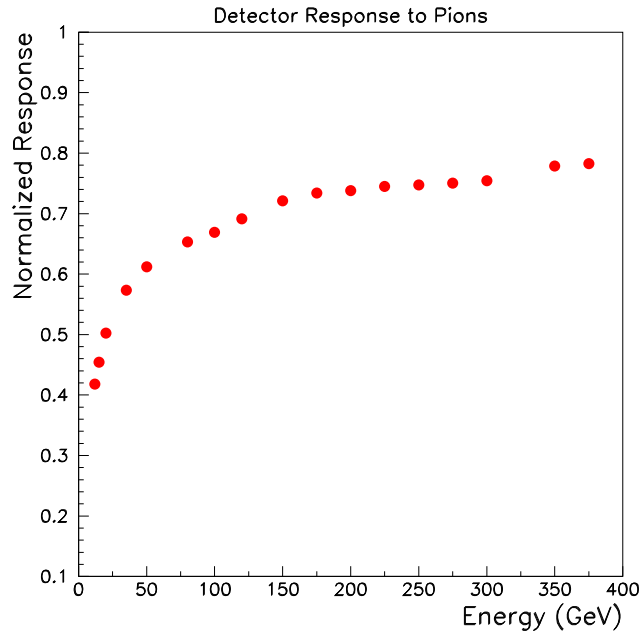


Figure 11: Normalized response to  $\pi^-$ s as a function of beam energy

energy resolution was determined to be 20% at 1 TeV. The response was found to be linear to 1% for electrons. A highly non-linear behavior for hadrons was observed.

## 5 Acknowledgment

We would like to thank our colleagues from CMS in particular J. Bourotte and M. Haguenaer for their assistance in the various tests described in this paper. We also thank Jim Freeman, Dan Green, and Andris Skuja from CMS for their encouragement and support. This work was supported by the US Department of Energy (DE-FG02-91ER-40664) and NSF (NSF-JNT-98-20258), the Hungarian National Fund (OTKA T026184), the International Science Foundation (grants M 82000 and M 82300), the State Committee of the Russian Federation for Science and Technologies, and the Russian Research Foundation (grant 95-02-04815) and the Scientific and Technical Research Council of Turkey (TUBITAK)

## References

- [1] The CMS Collaboration. Technical Proposal. CERN/LHCC 94-39, 1994.n
- [2] The CMS Collaboration, *The Hadron Calorimeter Project Technical Design Report*, CERN/LHCC 97-31 (1997).
- [3] R. Wigmans, *Calorimetry: Energy Measurement In Particle Physics*, Oxford University Press, 2000.
- [4] M.J. Berger and S.M. Seltzer, *Tables of Energy Loses and Ranges of Electrons and Positrons*, NASA Report NASA-SP-3012, 1964.
- [5] J.V. Jelly, *Čerenkov Radiation and Its Applications*, Pergamon Press, 1958.
- [6] N. Akchurin et al., *Nucl. Instr. and Meth.* **A399** (1997) 202.
- [7] T.S. Virdee, *Techniques and Concepts of High Energy Physics X*, T. Ferbel ed., NATO Science Series C, Vol. 534
- [8] N. Akchurin et al., *Nucl. Instr. and Meth.* **A409** (1998) 593.
- [9] N. Akchurin et al., *Nucl. Instr. and Meth.* **A408** (1998) 380.
- [10] N. Akchurin et al., *Nucl. Instr. and Meth.* **A400** (1997) 267.
- [11] N. Akchurin et al., *Nucl. Instr. and Meth.* **A379** (1996) 526.